INTERNATIONAL JOURNAL FOR NUMERICAL METHODS IN FLUIDS
Int. J. Numer. Meth. Fluids **29**: 265–288 (1999)

NUMERICAL SOLUTION FOR THE SECOND-ORDER WAVE INTERACTION WITH POROUS STRUCTURES

HU-HSIAO HSU AND YUNG-CHAO WU*

Department of Civil Engineering, National Chiao-Tung University, Hsinchu, Taiwan, Province of China

SUMMARY

This study mathematically formulates the fluid field of a water-wave interaction with a porous structure as a two-dimensional, non-linear boundary value problem (bvp) in terms of a generalized velocity potential. The non-linear bvp is reformulated into an infinite set of linear bvps of ascending order by Stokes perturbation technique, with wave steepness as the perturbation parameter. Only the first- and second-order linear bvps are retained in this study. Each linear bvp is transformed into a boundary integral equation. In addition, the boundary element method (BEM) with linear elements is developed and applied to solve the first- and second-order integral equations. The first- and second-order wave profiles, reflection and transmission coefficients, and the amplitude ratio of the second-order components are computed as well. The numerical results correlate well with previous analytical and experimental results. Numerical results demonstrate that the second-order component can be neglected for a deep water-wave and may become significant for an intermediate depth wave. Copyright © 1999 John Wiley & Sons, Ltd.

KEY WORDS: boundary element method; porous structure; reflection coefficient; transmission coefficient

1. INTRODUCTION

In ocean engineering, porous structures such as rubble-mound breakwaters have been widely constructed to protect harbors, inlets and beaches from wave action. Porous structures provide shelter from wave attack by reflecting and dissipating incident wave energy. These structures are also frequently used as absorbers in laboratories to remove unwanted waves during experiments. In addition, the functional efficiency of these structures can be evaluated by calculating the reflection and transmission of waves. In permeable breakwaters, a portion of the incident wave energy is transmitted through the porous structure. Water depth, as well as wave properties such as wave period and wave height, and structural properties markedly influence the distribution of reflected, transmitted and dissipated wave energies. The major structural properties are geometry, porosity, permeability, size distribution and shape function of the components of the porous structures.

The interaction among progressing waves and a porous structure can be addressed in several ways. Previous investigations have derived theoretical solutions for the reflection and transmission coefficients by using eigenfunction expansions in the fluid and in the porous structure [1–4]. However, their solutions are valid only for structures with rectangular cross-sections

* Correspondence to: Department of Civil Engineering, National Chiao-Tung University, Hsinchu, Taiwan, Province of China.

CCC 0271–2091/99/030265–24$17.50

Received 6 September 1996
Revised 4 September 1997

under normally incident linear waves. Dalrymple *et al*. [5] extended the solutions to structures subjected to an oblique wave attack. Recently, Lee and Lan [6] analyzed the porous structural problems up to the second-order. These investigators also analyzed trapezoidal breakwaters by considering an equivalent breakwater of rectangular cross-section [1,4] or by boundary element models [7].

In addition to the above efforts, other scholars have closely examined the porous problems using various methods. Chwang [8] applied Taylor's [9] concept of a porous screen to avert the complicated porous structure flow and develop the so-called porous wavemaker theory. Huang and Chao [10] proposed a solution involving the porous Reynolds number, thereby avoiding the complex bvp. Owing to the problem's complexity, experimental studies are considered indispensable tools in providing reliable information for engineering applications, Iwasaki and Numata [11], Dattatri *et al*. [12], Aminti and Franco [13] and Oumeraci and Partensucky [14]. However, such results are restricted only to specific types of porous structures.

In this study, a generalized potential theory is applied to describe both water and porous flow regions. The original non-linear boundary value problem (bvp) is linearized by the perturbation method. The numerical solutions are derived up to the second-order. The boundary element method (BEM) is used to solve the first- and second-order bvps. An attempt is also made to increase the numerical solution's accuracy by using the linear element to perform computations. Moreover, the numerical solution's accuracy is demonstrated by comparing the analytical solution and the experimental data.

2. THEORETICAL FORMULATION OF THE PROBLEM

Herein, the interaction of a gravity wave train with a single homogeneous, isotropic, porous structure of width b, between two semi-infinite fluid regions of constant depth h, as shown in Figure 1, is considered. A Cartesian co-ordinate is chosen with the origin located at the still water surface. The porous structure is specified with given porous features and is considered to be rectangular with a horizontal bottom. The incident wave is specified propagating in the $+x$-direction, with a wave height H and a period T. The incident wave train encountering the porous structure face is partially reflected and partially transmitted. The wave motion inside the porous structure decays as it propagates through the pores. Then, as it encounters the leeward structural face, it is partially reflected back into the structure and partially transmitted into the leeward semi-infinite fluid region. Inside the porous structure, the transmitted and reflected waves are subsequently reflected and transmitted back and forth between the two outside faces.

To resolve the above problem, the domain is divided into three regions, i.e. a porous structure region and two water regions in front of and behind the porous structure. In this study, the mathematical model used to describe the flow regions for the porous structure and water regions is generalized into one theory. Only the flow mechanism in the porous structure is mathematically described.

By making the usually assumptions of classical hydrodynamics, the wave field outside the structure can be specified by velocity potentials [1], Φ_1 in the seaward region (denoted region 1) and Φ_3 in the leeward region of the porous structure (region 3). In the porous structure, the incompressible fluid motion for the discharge velocity is also describable by a potential (Φ_2), and a modified free-surface boundary condition. The velocity potentials $\Phi_j(x, z, t)$ can be expressed as:

$$\Phi_j(x, z, t) = \text{Real}[\phi_j(x, z)\, e^{-i\omega t}], \quad j = 1, 2, 3, \tag{1}$$

where $i = \sqrt{-1}$, and the velocity potentials $\phi_j(x, z)$ must satisfy the Laplace equation

$$\nabla^2 \phi_j = 0. \tag{2}$$

The unsteady Bernoulli equation for the flow in the porous structure can be expressed as [1,6]:

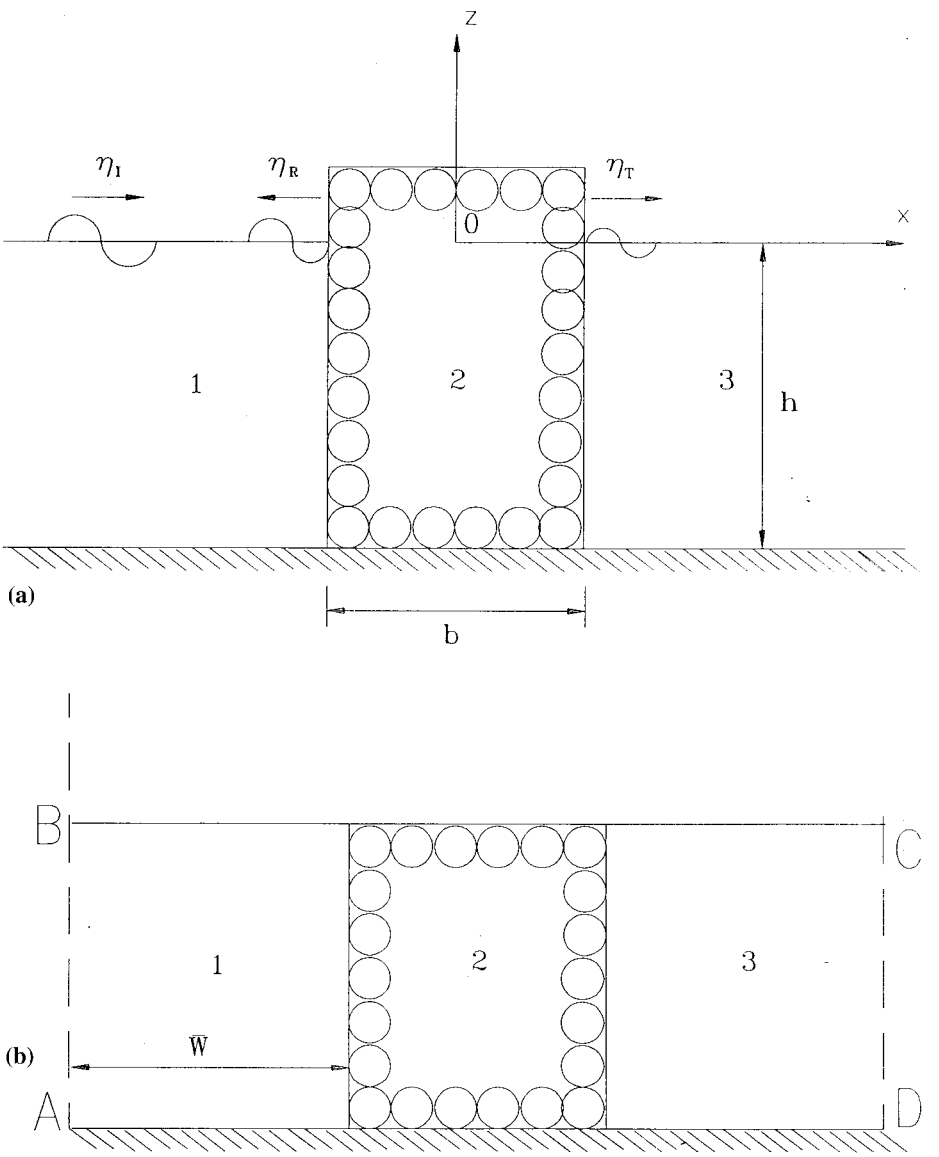

Figure 1. Schematic diagram of waves propagating over a porous structure; (a) physical domain; (b) computational domain.

$$-S_j\frac{\partial\Phi_j}{\partial t}+\frac{S_j}{2}\left[\left(\frac{\partial\Phi_j}{\partial x}\right)^2+\left(\frac{\partial\Phi_j}{\partial z}\right)^2\right]+\frac{P_j}{\rho}+gz-\omega f_j\Phi_j=0, \tag{3}$$

where the subscript j denotes the jth flow region, S_j represents the virtual mass coefficient, ρ is the fluid density, g denotes the gravity acceleration, and ω represents the wave frequency. The final term of the left-hand side of Equation (3) represents the flow resistance and f_j is referred to as the friction coefficient. In addition, the friction coefficient f_j is defined by using the Lorentz condition of equivalent work, and can be written as [15]:

$$f_j=\frac{1}{\omega}\left\{\frac{\varepsilon_j v}{K_{pj}}+\frac{\varepsilon_j^2 C_{fj}}{\sqrt{K_{pj}}}\frac{\int_\forall\int_t^{t+T}|\vec{V}_j|^3\,\mathrm{d}t\,\mathrm{d}\forall}{\int_\forall\int_t^{t+T}|\vec{V}_j|^2\,\mathrm{d}t\,\mathrm{d}\forall}\right\}, \tag{4}$$

where $\vec{V}_j$ denotes the real part of the seepage velocity, v represents the kinematic fluid viscosity, C_{fj} denotes the turbulence drag coefficient, ε_j is the porosity of the medium, and K_{pj} represents the intrinsic permeability of the porous medium. For $S_j=1$ and $f_j=0$, Equation (3) is reduced to the well-known Bernoulli equation for the irrotational flow of an ideal fluid.

Equations (3) and (4) indicate that the non-linearity of the flow resistance is maintained in an implicit form. In the solution, the problem is iteratively solved by assuming a friction f_j value, which is then recalculated from the solved flow velocity. In the first-order solution, the linear velocity is used to calculate the friction coefficient. However, in the second-order solution, the linear velocity and the second-order component of the velocity are used to calculate the friction coefficient. Furthermore, the use of Equation (3) implies irrotational flow and the generalized velocity potential function exists. A theoretical proof was given by Lee [4].

Figure 1(a) depicts the physical domain of the present problem. The porous structure is subjected to incident waves with frequency ω and wave height H. The first region includes incident waves Φ_1^{I} and reflected waves Φ_1^{R}, and the third region contains transmitted waves Φ_3^{T}. Based on the above theoretical framework, the boundary conditions for the jth region (Figure 1) are given below.

1. The kinematic free-surface boundary condition:

$$\frac{\partial\eta_j}{\partial t}+\frac{\partial\Phi_j}{\partial z}-\frac{\partial\eta_j}{\partial x}\frac{\partial\Phi_j}{\partial x}=0 \quad \text{on} \quad z=\eta_j; \qquad j=1,2,3. \tag{5}$$

2. The dynamic free-surface boundary condition:

$$-S_j\frac{\partial\Phi_j}{\partial t}+\frac{S_j}{2}\left[\left(\frac{\partial\Phi_j}{\partial x}\right)^2+\left(\frac{\partial\Phi_j}{\partial z}\right)^2\right]+g\eta_j-\omega f_j\Phi_j=0 \quad \text{on} \quad z=\eta_j. \tag{6}$$

3. The boundary condition at the water bottom:

$$\frac{\partial\Phi_j}{\partial\vec{n}}=0 \quad \text{on} \quad z=-h, \tag{7}$$

   indicates that the bottom is impermeable. The vector $\vec{n}$ is the unit normal vector pointing out of the computation domain.
4. The radiation conditions: These conditions model the behavior of an outgoing wave at a distance far away from the structure (where the water depth remains constant).
5. The matching boundary conditions at the interface of the $(j-1)$th and jth regions $(j=2,3)$:

$$\varepsilon_{(j-1)}\frac{\partial\Phi_{(j-1)}}{\partial x}=\varepsilon_j\frac{\partial\Phi_j}{\partial x}, \tag{8}$$

$$-S_{(j-1)}\frac{\partial\Phi_{(j-1)}}{\partial t}+\frac{S_{(j-1)}}{2}\left[\left(\frac{\partial\Phi_{(j-1)}}{\partial x}\right)^2+\left(\frac{\partial\Phi_{(j-1)}}{\partial z}\right)^2\right]-\omega f_{(j-1)}\Phi_{(j-1)}$$
$$=-S_j\frac{\partial\Phi_j}{\partial t}+\frac{S_j}{2}\left[\left(\frac{\partial\Phi_j}{\partial x}\right)^2+\left(\frac{\partial\Phi_j}{\partial z}\right)^2\right]-\omega f_j\Phi_j. \tag{9}$$

These equations can be applied to pure fluid regions, $j=1$ and $j=3$, by specifying the virtual mass coefficient to be unity ($S_j=1$) and the friction coefficient to be zero ($f_j=0$) in the equations.

The resulting non-linear bvp can be reformulated using a perturbation method. With the perturbation approach, it is assumed that the solution relies on the presumed small quantity ϵ, the wave steepness. The series form of the velocity potential can be written as [16]:

$$\Phi_j(x,z,t)=\sum_{n=1}^{\infty}\Phi_{jn}(x,z,t), \tag{10}$$

where a perturbation parameter, ϵ, is implicitly included in the expansion. Other physical quantities such as dynamic pressure, surface elevation and velocities can also be similarly expanded. The fact that the location of the water surface is *a priori* unknown accounts for why the free-surface boundary conditions must also be expanded in the Taylor series around the still water level.

By applying the perturbation procedures, the bvps of the first- and second-order are formulated. The first-order bvp can be expressed as:

$$\nabla^2\Phi_{j1}=0,\quad j=1,2,3, \tag{11}$$

$$S_j\frac{\partial^2\Phi_{j1}}{\partial t^2}+g\frac{\partial\Phi_{j1}}{\partial z}+\omega f_j\frac{\partial\Phi_{j1}}{\partial t}=0\quad\text{on}\quad z=0, \tag{12}$$

$$\frac{\partial\Phi_{j1}}{\partial z}=0\quad\text{on}\quad z=-h. \tag{13}$$

The matching boundary conditions on the interface of the $(j-1)$th and jth regions ($j=2,3$), are

$$\varepsilon_{(j-1)}\frac{\partial\Phi_{(j-1)1}}{\partial x}=\varepsilon_j\frac{\partial\Phi_{j1}}{\partial x}, \tag{14}$$

$$S_{(j-1)}\frac{\partial\Phi_{(j-1)1}}{\partial t}+\omega f_{(j-1)}\Phi_{(j-1)1}=S_j\frac{\partial\Phi_{j1}}{\partial t}+\omega f_j\Phi_{j1} \tag{15}$$

and radiation conditions, i.e. an outgoing wave at far-field.

The free-surface elevation can be computed according to the linearized Bernoulli equation evaluated at the free-surface:

$$\eta_{j1}=\frac{1}{g}\left\{S_j\frac{\partial\Phi_{j1}}{\partial t}+\omega f_j\Phi_{j1}\right\}\quad\text{on}\quad z=0, \tag{16}$$

which is identical to the linear problem given by Sollitt and Cross [1].

The second-order bvp can be expressed as:

$$\nabla^2\Phi_{j2}=0,\quad j=1,2,3, \tag{17}$$

$$S_j \frac{\partial^2 \Phi_{j2}}{\partial t^2} + g \frac{\partial \Phi_{j2}}{\partial z} + \omega f_j \frac{\partial \Phi_{j2}}{\partial t} = -S_j \eta_{j1} \frac{\partial^3 \Phi_{j1}}{\partial z\, \partial t^2} - \omega f_j \eta_{j1} \frac{\partial^2 \Phi_{j1}}{\partial z\, \partial t} - S_j \frac{\partial \eta_{j1}}{\partial t} \frac{\partial^2 \Phi_{j1}}{\partial z\, \partial t}$$
$$- \omega f_j \frac{\partial \eta_{j1}}{\partial t} \frac{\partial \Phi_{j1}}{\partial z} + S_j \frac{\partial \Phi_{j1}}{\partial x} \frac{\partial^2 \Phi_{j1}}{\partial x\, \partial t} + S_j \frac{\partial \Phi_{j1}}{\partial z} \frac{\partial^2 \Phi_{j1}}{\partial z\, \partial t}$$
$$+ g \frac{\partial \eta_{j1}}{\partial x} \frac{\partial \Phi_{j1}}{\partial x} - g \eta_{j1} \frac{\partial^2 \Phi_{j1}}{\partial z^2} \quad \text{on} \quad z = 0, \tag{18}$$

$$\frac{\partial \Phi_{j2}}{\partial z} = 0 \quad \text{on} \quad z = -h. \tag{19}$$

The matching boundary conditions at the interface of the $(j-1)$th and jth regions ($j = 2, 3$), are

$$\varepsilon_{(j-1)} \frac{\partial \Phi_{(j-1)2}}{\partial x} = \varepsilon_j \frac{\partial \Phi_{j2}}{\partial x}, \tag{20}$$

$$S_{(j-1)} \frac{\partial \Phi_{(j-1)2}}{\partial t} + \omega f_{(j-1)} \Phi_{(j-1)2} - \frac{S_{(j-1)}}{2} \left[\left(\frac{\partial \Phi_{(j-1)1}}{\partial x} \right)^2 + \left(\frac{\partial \Phi_{(j-1)1}}{\partial z} \right)^2 \right]$$
$$= S_j \frac{\partial \Phi_{j2}}{\partial t} + \omega f_j \Phi_{j2} - \frac{S_j}{2} \left[\left(\frac{\partial \Phi_{j1}}{\partial x} \right)^2 + \left(\frac{\partial \Phi_{j1}}{\partial z} \right)^2 \right] \tag{21}$$

and radiation conditions, i.e. an outgoing wave at far-field.

The free-surface elevation at $z = 0$ can be computed from the second-order Bernoulli equation:

$$\eta_{j2} = \frac{1}{g} \left\{ S_j \frac{\partial \Phi_{j2}}{\partial t} + \omega f_j \Phi_{j2} + S_j \eta_{j1} \frac{\partial^2 \Phi_{j1}}{\partial z\, \partial t} + \omega f_j \eta_{j1} \frac{\partial \Phi_{j1}}{\partial z} - \frac{S_j}{2} \left[\left(\frac{\partial \Phi_{j1}}{\partial x} \right)^2 + \left(\frac{\partial \Phi_{j1}}{\partial z} \right)^2 \right] \right\}. \tag{22}$$

The non-homogeneous terms in Equations (18) and (21) involve the products of the first-order solutions. Although complex variables are used in the expression of the linear solution, only the real part represents physical quantities. Therefore, redundant results attributed to multiplication of the imaginary parts should be excluded. By using Vantorre's expression [17], Equations (18), (21) and (22) can be reformulated into a time-dependent term proportional to $e^{-i2\omega t}$ and a time-independent term. The second-order velocity potential and surface elevation can be written in the form

$$\Phi_{j2}(x, z, t) = \phi_{j2}(x, z)\, e^{-i2\omega t} + \varphi_{j2}(x, z), \tag{23}$$

$$\eta_{j2}(x, t) = \hat{\eta}_{j2}(x)\, e^{-i2\omega t} + \tilde{\eta}_{j2}(x). \tag{24}$$

Equations (17)–(22), can be decomposed into two bvps: a time-dependent problem, $\phi_{j2}(x, z)$, and a time-independent problem, $\varphi_{j2}(x, z)$. In addition, the bvp for the time-dependent part of the second-order solution can be written as:

$$\nabla^2 \phi_{j2} = 0, \tag{25}$$

$$-2\omega^2 (2S_j + i f_j) \phi_{j2} + g \frac{\partial \phi_{j2}}{\partial z} = D_j(x) \quad \text{on} \quad z = 0, \tag{26}$$

$$\frac{\partial \phi_{j2}}{\partial z} = 0 \quad \text{on} \quad z = -h, \tag{27}$$

where $D_j(x)$ denotes

$$D_j(x) = \frac{\omega^5(-i3S_j + 2f_j)(S_j + if_j)^2}{2g^2}(\phi_{j1})^2 + \frac{\omega(-i2S_j + f_j)}{2}\left(\frac{\partial \phi_{j1}}{\partial x}\right)^2 + \frac{\omega(-iS_j + f_j)}{2}\phi_{j1}\frac{\partial^2 \phi_{j1}}{\partial x^2}. \tag{28}$$

The matching boundary conditions at the interface of the $(j-1)$th and jth regions ($j = 2, 3$), are

$$\varepsilon_{(j-1)}\frac{\partial \phi_{(j-1)2}}{\partial x} = \varepsilon_j \frac{\partial \phi_{j2}}{\partial x}, \tag{29}$$

$$\omega[-i2S_{(j-1)} + f_{(j-1)}]\phi_{(j-1)2} - \frac{S_{(j-1)}}{4}\left[\left(\frac{\partial \phi_{(j-1)1}}{\partial x}\right)^2 + \left(\frac{\partial \phi_{(j-1)1}}{\partial z}\right)^2\right] = \omega[-i2S_j + f_j]\phi_{j2} - \frac{S_j}{4}\left[\left(\frac{\partial \phi_{j1}}{\partial x}\right)^2 + \left(\frac{\partial \phi_{j1}}{\partial z}\right)^2\right]. \tag{30}$$

In region 1, the time-dependent potential function contains the second-order incident wave ϕ_{12}^{I} and *a priori* unknown reflected wave ϕ_{12}^{R}. The second-order time-dependent free-surface elevation at $z = 0$ can be expressed as

$$\hat{\eta}_{j2} = \frac{1}{g}\left\{\omega(-i2S_j + f_j)\phi_{j2} - \frac{S_j}{4}\left[\left(\frac{\partial \phi_{j1}}{\partial x}\right)^2 + \left(\frac{\partial \phi_{j1}}{\partial z}\right)^2\right] + \frac{-\omega^4(S_j + if_j)^3}{2g}(\phi_{j1})^2\right\}. \tag{31}$$

The bvp, Equations (25)–(30), in terms of ϕ_{j2} contains non-homogeneous boundary conditions, i.e. Equations (26), (29) and (30). To facilitate the solution of the problem, it is further decomposed into two parts: a Stokes wave problem, ϕ_{j2}^{s}, and a free-wave problem, ϕ_{j2}^{f}.

$$\phi_{j2} = \phi_{j2}^{\mathrm{s}} + \phi_{j2}^{\mathrm{f}}, \tag{32}$$

where ϕ_{j2}^{s} must satisfy Equations (25)–(27). The ϕ_{j2}^{f} must satisfy Equations (25) and (27), the radiation conditions and a homogeneous free-surface boundary condition [18].

The bvp for the time-independent part of the second-order solution can be expressed as:

$$\nabla^2 \varphi_{j2} = 0, \tag{33}$$

$$g\frac{\partial \varphi_{j2}}{\partial z} = E_j(x) \quad \text{on} \quad z = 0, \tag{34}$$

$$\frac{\partial \varphi_{j2}}{\partial z} = 0 \quad \text{on} \quad z = -h, \tag{35}$$

in which $E_j(x)$ can be expressed as

$$E_j(x) = \frac{i\omega^5 S_j(S_j + if_j)(S_j - if_j)}{2g^2}\phi_{j1}\bar{\phi}_{j1} + \frac{\omega f_j}{2}\frac{\partial \phi_{j1}}{\partial x}\frac{\partial \bar{\phi}_{j1}}{\partial x} + \frac{\omega(-iS_j + f_j)}{2}\phi_{j1}\frac{\partial^2 \bar{\phi}_{j1}}{\partial x^2}, \tag{36}$$

where $\bar{\phi}_{j1}$, $\partial \bar{\phi}_{j1}/\partial x$ and $\partial^2 \bar{\phi}_{j1}/\partial x^2$ represent the complex conjugate of ϕ_{j1}, $\partial \phi_{j1}/\partial x$ and $\partial^2 \phi_{j1}/\partial x^2$ respectively. The matching boundary conditions between the $(j-1)$th and jth regions ($j = 2, 3$) are

$$\varepsilon_{(j-1)}\frac{\partial \varphi_{(j-1)2}}{\partial x} = \varepsilon_j \frac{\partial \varphi_{j2}}{\partial x}, \tag{37}$$

$$-\omega f_{(j-1)}\varphi_{(j-1)2}+\frac{S_{(j-1)}}{4}\left[\left(\frac{\partial\phi_{(j-1)1}}{\partial x}\right)\left(\frac{\partial\bar{\phi}_{(j-1)1}}{\partial x}\right)+\left(\frac{\partial\phi_{(j-1)1}}{\partial z}\right)\left(\frac{\partial\bar{\phi}_{(j-1)1}}{\partial z}\right)\right]$$
$$=-\omega f_j\varphi_{j2}+\frac{S_j}{4}\left[\left(\frac{\partial\phi_{j1}}{\partial x}\right)\left(\frac{\partial\bar{\phi}_{j1}}{\partial x}\right)+\left(\frac{\partial\phi_{j1}}{\partial z}\right)\left(\frac{\partial\bar{\phi}_{j1}}{\partial z}\right)\right], \tag{38}$$

where $\partial\bar{\phi}_{j1}/\partial z$ denotes the complex conjugate of $\partial\phi_{j1}/\partial z$. The time-independent part of the corresponding free-surface elevation at $z=0$ can be expressed as

$$\tilde{\eta}_{j2}=\frac{1}{g}\left\{-\frac{S_j}{4}\left[\frac{\partial\phi_{j1}}{\partial x}\frac{\partial\bar{\phi}_{j1}}{\partial x}+\frac{\partial\phi_{j1}}{\partial z}\frac{\partial\bar{\phi}_{j1}}{\partial z}\right]+\omega f_j\varphi_{j2}+\frac{-\omega^4(S_j+if_j)^3}{2g}\phi_{j1}\bar{\phi}_{j1}\right\}. \tag{39}$$

The procedures to solve the time-dependent bvp can be applied herein to resolve the time-independent bvp φ_{j2}. Moreover, the solution can be written as the sum of a solution of a bvp, $\varphi^{\mathrm{s}}_{j2}$, and a solution of a bvp, $\varphi^{\mathrm{f}}_{j2}$, i.e.

$$\varphi_{j2}=\varphi^{\mathrm{s}}_{j2}+\varphi^{\mathrm{f}}_{j2}, \tag{40}$$

where $\varphi^{\mathrm{s}}_{j2}$ must satisfy Equations (33)–(35). Also, $\varphi^{\mathrm{f}}_{j2}$ must satisfy Equations (33) and (35), the radiation conditions and a homogeneous free-surface boundary condition [19].

3. OPEN BOUNDARY TREATMENT

At far-field, $x=\pm(\bar{W}+(b/2))$, the radiation conditions stipulate that both the reflection wave and the transmission wave propagate away from the porous structure. Therefore, the following discussion encompasses the velocity potentials, the first- and second-order, which satisfy governing equation and radiation conditions in the region of constant depth, h. The first-order velocity potential at the reflection side that satisfies Equations (11)–(13) and the radiation condition, can be expressed as [18]:

$$\Phi^{\mathrm{r}}_1(x,z,t)=\phi^{\mathrm{r}}_1(x,z)\,\mathrm{e}^{-i\omega t}, \tag{41}$$

$$\phi^{\mathrm{r}}_1=\frac{gH}{2\omega}\frac{\cosh[k(h+z)]}{\cosh kh}\exp[ik(x+\bar{W}+(b/2))]$$
$$+\frac{gH_{\mathrm{r}}}{2\omega}\frac{\cosh[k(h+z)]}{\cosh kh}\exp[-ik(x+\bar{W}+(b/2))]+\text{evanescent modes}. \tag{42}$$

The subscript represents the order of magnitude. The first term is the velocity potential of the first-order incident wave; the second term is the velocity potential of the first-order reflection wave, where H_{r} denotes the wave height of the reflection wave. The last term decays away to zero at far-field, $\bar{W}=6h$ and therefore, is neglected herein. In addition, k and ω must satisfy the dispersion relation,

$$\omega^2=gk\tanh kh. \tag{43}$$

At interface AB (Figure 1(b)), $x=-(\bar{W}+(b/2))$, the matching conditions provide continuity of pressures and horizontal velocities normal to the vertical interface. The relation between velocity potential, ϕ_{11}, and normal velocity, $\partial\phi_{11}/\partial n$, on the vertical interface AB is derived in Appendix A (Equation (69)). In the present context, it can be written as

$$\phi_{11}=H\frac{g}{\omega}\frac{\cosh k(h+z)}{\cosh kh}+\frac{\cosh k(h+z)}{ikQ_0}\int_{-h}^{0}\frac{\partial\phi_{11}}{\partial n}\cosh k(h+z)\,\mathrm{d}z. \tag{44}$$

Similarly, on the vertical interface CD ($x = (\bar{W} + (b/2))$), the relation between ϕ_{31} and $\partial\phi_{31}/\partial n$ can be established as (Appendix A)

$$\phi_{31} = \frac{\cosh k(h+z)}{ikQ_0} \int_{-h}^{0} \frac{\partial \phi_{31}}{\partial n} \cosh k(h+z)\, \mathrm{d}z. \tag{45}$$

The time-dependent velocity potential, $\Phi_2^{\mathrm{rs}} = \phi_2^{\mathrm{rs}}\, \mathrm{e}^{-i2\omega t}$, at the reflection side of the second-order Stokes wave can be analytically solved as [18]:

$$\phi_2^{\mathrm{rs}} = i\left[\frac{gk}{4\omega}\frac{(2\cosh(2kh)-1)}{2\sinh(2kh)}\right] HH_{\mathrm{r}} + (-i)\frac{3\omega}{32}\frac{\cosh[2k(h+z)]}{\sinh^4(kh)} H^2 \exp[i2k(x+\bar{W}+(b/2))] + (-i)\frac{3\omega}{32}\frac{\cosh[2k(h+z)]}{\sinh^4(kh)} H_{\mathrm{r}}^2 \exp[-i2k(x+\bar{W}+(b/2))] + \text{evanescent modes}. \tag{46}$$

The first term is due to the interaction of the first-order incident wave and the first-order reflection wave; the second term is the velocity potential of the second-order Stokes incident wave, the third term is attributed to the interaction of the first-order reflection wave. The final term decays away to zero at far-field and is therefore, neglected herein.

The time-dependent velocity potential $\Phi_2^{\mathrm{rf}} = \phi_2^{\mathrm{rf}}\, e^{-i2\omega t}$ at the reflection side of the second-order free-wave can be expressed as [18]:

$$\phi_2^{\mathrm{rf}} = \bar{A} \cosh \beta(h+z) \exp[-i\beta(x+\bar{W}+(b/2))] + \text{evanescent modes}, \tag{47}$$

where $\bar{A}$ is an unknown coefficient. Evanescent modes decay away to zero at far-field. β and ω must satisfy the dispersion relation

$$(2\omega)^2 = g\beta \tanh \beta h. \tag{48}$$

Similarly, at interface AB, using the matching conditions provides continuity of pressures and horizontal velocities normal to the vertical interface. The open boundary condition can be expressed as (Appendix B):

$$\phi_{12} = R_1(z) + \frac{-i\cosh\beta(h+z)}{\beta W_0} \int_{-h}^{0} \frac{\partial \phi_{12}}{\partial n} \cosh \beta(h+z)\, \mathrm{d}z. \tag{49}$$

On the transmission side,

$$\phi_2^{\mathrm{ts}} = \frac{-i3\omega}{32\sinh^4 kh} H_{\mathrm{t}}^2 \cosh 2k(h+z) \exp[i2k(x-\bar{W}-(b/2))] + \text{evanescent modes} \tag{50}$$

and

$$\phi_2^{\mathrm{tf}} = \bar{B} \cosh \beta(h+z) \exp[i\beta(x-\bar{W}-(b/2))] + \text{evanescent modes}, \tag{51}$$

where $\bar{B}$ denotes an unknown coefficient. The relation between ϕ_{32} and ϕ_{32n} on the interface CD ($x = (\bar{W} + (b/2))$) can be established as (Appendix B):

$$\phi_{32} = R_2(z) + \frac{-i\cosh\beta(h+z)}{\beta W_0} \int_{-h}^{0} \frac{\partial \phi_{32}}{\partial n} \cosh \beta(h+z)\, \mathrm{d}z. \tag{52}$$

The time-independent velocity potential, φ_2^{rs}, at the reflection side of the second-order wave can be analytically solved [19], i.e.

$$\varphi_2^{\mathrm{rs}} = \frac{i\omega}{32}\left(\frac{3}{\sinh^2 kh} + \frac{1}{\cosh^2 kh}\right) H\bar{H}_{\mathrm{r}} \cosh 2k(h+z) \exp[i2k(x + \bar{W} + (b/2))] + \frac{i\omega}{32}\left(\frac{3}{\sinh^2 kh} + \frac{1}{\cosh^2 kh}\right) \bar{H}H_{\mathrm{r}} \cosh 2k(h+z) \exp[-i2k(x + \bar{W} + (b/2))]. \tag{53}$$

The time-independent velocity potential, φ_2^{rf}, at the reflection side of the second-order wave can be expressed as [19]:

$$\varphi_2^{\mathrm{rf}} = \bar{C}x + \sum_{n=1}^{\infty} \hat{A}_n \cos \mu_n(h+z) \exp[\mu_n(x + \bar{W} + (b/2))], \quad \mu_n = \frac{n\pi}{h}, \quad n = 1, 2, 3, \ldots, \tag{54}$$

based on the assumption of no-uniform current, i.e. $\bar{C} = 0$, and the series summation term decays away to zero at far-field. Therefore, at interface AB, $x = -(\bar{W} + (b/2))$

$$\varphi_{12} = \varphi_2^{\mathrm{rs}} + \varphi_2^{\mathrm{rf}} = \frac{i\omega}{32}\left(\frac{3}{\sinh^2 kh} + \frac{1}{\cosh^2 kh}\right) H\bar{H}_{\mathrm{r}} \cosh 2k(h+z) + \frac{i\omega}{32}\left(\frac{3}{\sinh^2 kh} + \frac{1}{\cosh^2 kh}\right) \bar{H}H_{\mathrm{r}} \cosh 2k(h+z). \tag{55}$$

Similarly, on the transmission side,

$$\varphi_2^{\mathrm{ts}} = 0 \tag{56}$$

and

$$\varphi_2^{\mathrm{tf}} = \bar{K}x + \sum_{n=1}^{\infty} \hat{B}_n \cos \mu_n(h+z) \exp[-\mu_n(x - \bar{W} - (b/2))], \tag{57}$$

assuming no-uniform current ($\bar{K} = 0$) exists and the series summation term decays away to zero at far-field. Therefore, at interface CD, $x = (\bar{W} + (b/2))$

$$\varphi_{32} = \varphi_2^{\mathrm{ts}} + \varphi_2^{\mathrm{tf}} = 0. \tag{58}$$

Equations (44), (45), (49), (52), (55) and (58) are the open boundary conditions on AB and CD of Figure 1(b), which correspond to the first-order, the time-dependent part of the second-order and the time-independent part of the second-order problems respectively.

4. BEM FORMULATION

The BEM has been used to solve a variety of problems in theoretical hydrodynamics and elasticity theory [20]. For a bvp in which the free-space Green's function is known, the BEM can be used to perform computations only on the domain's boundary.

Utilizing the BEM initially involves converting the bvps into an integral equation representation. Using Green's second identity

$$\int_{\Gamma} \left(\hat{\phi}\frac{\partial q}{\partial \vec{n}} - q\frac{\partial \hat{\phi}}{\partial \vec{n}}\right) \mathrm{d}\Gamma = \int_{\Omega} (\hat{\phi}\nabla^2 q - q\nabla^2 \hat{\phi})\, \mathrm{d}\Omega, \tag{59}$$

where q denotes the fundamental solution of the governing equation, Γ represents the boundary of the solution domain, Ω is the solution domain, and $\hat{\phi}$ denotes the velocity potential at a selected point of the boundary.

The fact that the governing equation of the fluid domain is the Laplace equation accounts for why the fundamental solution is [21]

$$q = \frac{1}{2\pi} \ln\left(\frac{1}{r}\right), \tag{60}$$

where r represents the distance from the source point to the field point. From Equation (59) any velocity potential $\hat{\phi}_j$ of the boundary is given by

$$-\frac{\beta}{2\pi}\hat{\phi}_j = \int_\Gamma \left(\hat{\phi}\frac{\partial q}{\partial \vec{n}} - q\frac{\partial \hat{\phi}}{\partial \vec{n}}\right) \mathrm{d}\Gamma, \tag{61}$$

where j denotes the source point and β represents the internal angle of the source point j.

The numerical procedure of the BEM entails dividing the boundary into N segments or elements. To increase the numerical method's accuracy, the linear element is used to perform computations on the domain's boundary. Next, Equation (61) is numerically integrated using Gaussian quadrature. Finally, a system of N equations is established. The system of N equations can be written as

$$[H]\{\hat{\phi}\} = [G]\left\{\frac{\partial \hat{\phi}}{\partial n}\right\}, \tag{62}$$

in which $[H]$ and $[G]$ are known and rely only on the geometry. Therefore, instead of attempting to obtain the unknown distribution of the boundary values over the discretized surface, the problem is reduced to finding the unknown $\hat{\phi}$ and $\partial\hat{\phi}/\partial n$ at the nodal points.

In the previous section, the relation between $\hat{\phi}$ and $\partial\hat{\phi}/\partial n$ was established. Herein, the discretized forms of the open boundaries are established on the basis of linear element. By combining Equation (62) with the discretized form of the open boundary conditions, a sufficient number of equations exist to solve unknown quantities. After rearranging the equations in such a manner that all unknowns are taken to the left-hand side and all the knowns are moved to the right-hand side, Equation (62) can be written as:

$$[A][X] = [B], \tag{63}$$

where $[X]$ denotes the vector of unknown ϕ_{jm} and $\partial\phi_{jm}/\partial n$ $(m = 1, 2)$, $[B]$ represents the known vector and $[A]$ is the matrix of coefficients. Equation (63) can be solved by employing the Gauss elimination method.

5. NUMERICAL RESULTS AND DISCUSSION

This work has examined the second-order problem of the interaction of progressive wave and porous structure in water of constant depth by the BEM. To ensure the accuracy of the computation, the numerical solutions of the BEM are compared with available analytical solutions of Lee and Lan [6] and experimental results of Sollitt and Cross [1]. The friction coefficient used to describe the flow mechanism in the porous region is calculated by the Lorentz's condition [15] of equivalent work, i.e. Equation (4). In addition, the flow velocities of the first- and second-order are defined using the perturbation definition:

$$\text{The first order: } |\vec{V}_1| = \sqrt{\text{Real}\{u_{x21}\}^2 + \text{Real}\{u_{z21}\}^2} \tag{64}$$

$$\text{The second order: } |\vec{V}_2| = \sqrt{\text{Real}\{u_{x21} + u_{x22}\}^2 + \text{Real}\{u_{z21} + u_{z22}\}^2}, \tag{65}$$

where the first subscript of u represents velocity direction, the second subscript denotes flow region and the third subscript is the order of magnitude.

The reflection and transmission coefficients of the first- and second-order waves are defined as

$$K_{1r} = \sqrt{\frac{E_{1r}}{E_{1i}}} \quad K_{1t} = \sqrt{\frac{E_{1t}}{E_{1i}}}$$
$$K_{2r} = \sqrt{\frac{E_{2r}}{E_{2i}}} \quad K_{2t} = \sqrt{\frac{E_{2t}}{E_{2i}}} \tag{66}$$

where E_{1i}, E_{1r} and E_{1t} are the first-order energies of incident, reflected and transmitted waves respectively. Moreover, E_{2i}, E_{2r} and E_{2t} are the complete second-order total energies of incident, reflected and transmitted waves respectively.

Figure 2 presents the numerical solutions for wave steepness $H/L = 0.01$, dimensionless width of the porous structure $b/h = 1.0$, porosity $\varepsilon_2 = 0.439$, turbulence drag coefficient $C_{f2} = 0.295$, intrinsic permeability $K_{p2} = 0.1138 \times 10^{-5}$ (ft^2) and kinematic viscosity $\nu = 1.09 \times 10^{-5}$ (ft^2 s^{-1}). This figure also compares numerical results in this study with points taken from analytical results of Lee and Lan [6]. The results of this study closely correlate with those of Lee and Lan [6], with the only discrepancy found in the linear reflection coefficient. Next, the proposed numerical model's accuracy is confirmed by reanalyzing the linear problem by the method of matched eigenfunction expansion, as used by Lee and Lan [6]. The analytical solutions, plotted in Figure 2, closely correlate with the BEM solutions. Therefore, the proposed numerical model's accuracy is verified. Reasons for the discrepancy between this study and Lee and Lan [6] still remain unknown.

This study also considers two different wave steepnesses, $H/L = 0.01$ and 0.02, and two different porous structural properties (Table I). The first-order problems are solved by both the BEM and the analytical method; the second-order problems are solved by the BEM only. Figures 3–5 plot the numerical results.

Figures 3–5 present the reflection and transmission coefficients for a permeable breakwater of rectangular cross-section, as a function of relative water depth, kh. Notably, more wave energy is dissipated in the porous structure for a deeper water-wave. The effect of second-order is important in the region of intermediate depth wave, $\pi/10 < kh < \pi$. In addition, the importance of the second-order effect increases with an increasing wave steepness.

The surface elevation can be computed according to Equations (16) and (22). For $kh = 0.4$ and 1.0, Figures 6 and 7 display the temporal waveforms at four different locations. Each figure includes the temporal waveforms η^1, $\eta^1 + \eta^{2s}$ and $\eta^1 + \eta^{2s} + \eta^{2f}$, where η^1 denotes the first-order wave profile, η^{2s} represents the second-order Stokes' wave profile, and η^{2f} is the second-harmonic free-wave profile. These figures reveal that the surface elevations differ at different position. This phenomenon is attributed to the fact that the second-order free-wave moving with phase velocity is smaller than the Stokes' wave, (Equations (43) and (48)).

Figure 6, $kh = 0.4$, indicates that the second-order free-surface elevation, $\eta^1 + \eta^2$, has an obvious deformation, implying that the second-order component is important. On the other hand, Figure 7, $kh = 1.0$, indicates that the deformation of the second-order free-surface is insignificant, i.e. the second-order component can be neglected. Therefore, it can be concluded that the effect of second-order wave component gradually decreases with an increasing relative water depth. Herein, an attempt is also made to further understand the relative importance of

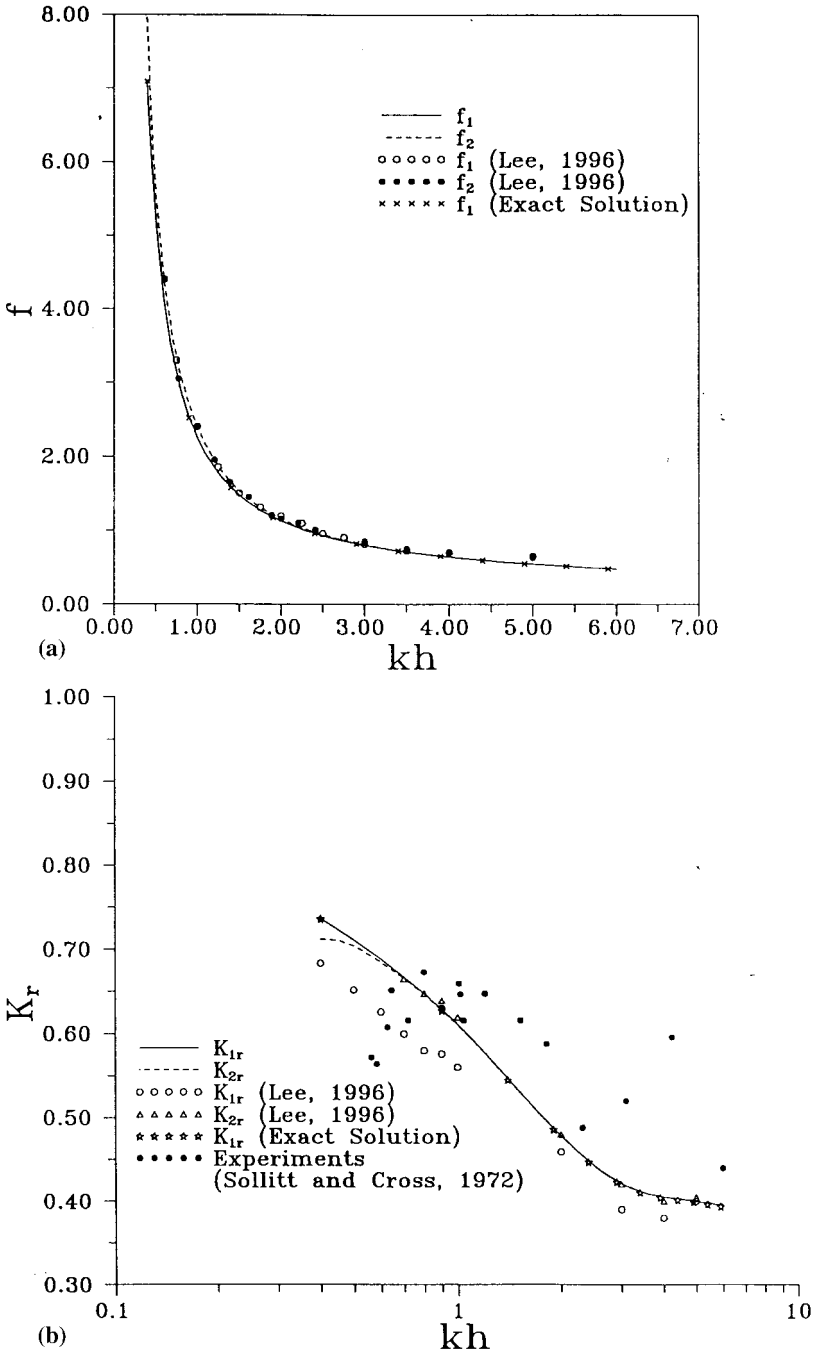

Figure 2. Friction (a), reflection (b) and transmission (c) coefficients ($H/L = 0.01$, $\varepsilon_2 = 0.439$, $K_{p2} = 0.1138 \times 10^{-5}$, $C_{f2} = 0.295$).

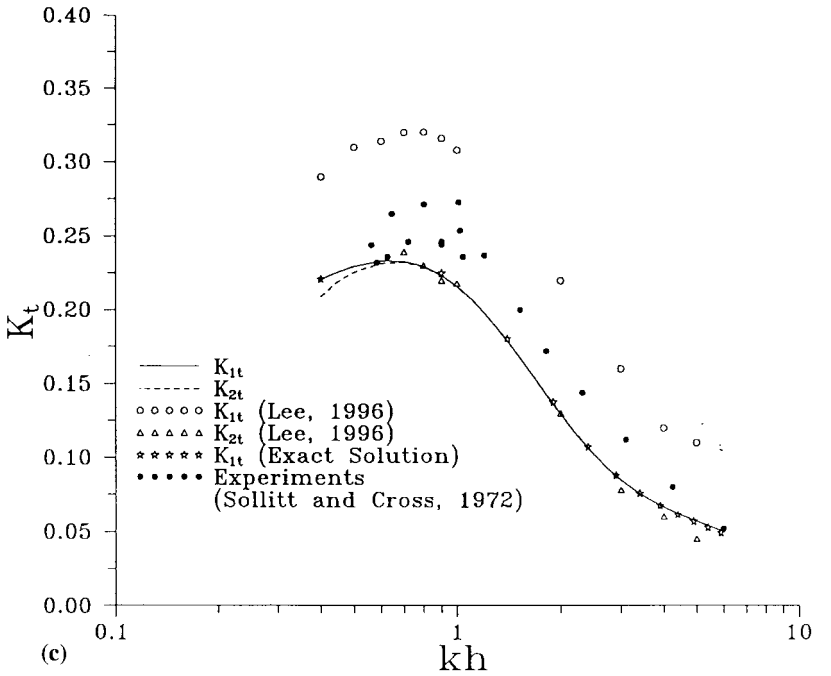

Figure 2 (*Continued*)

the second-harmonic free-wave and the second-order Stokes' wave. Figure 8 plots the ratio of free-wave amplitude and Stokes' wave amplitude, $|\eta^{2f}|/|\eta^{2s}|$ for different relative water depths. According to this figure, the second-harmonic free-wave is overwhelmingly larger than the Stokes' wave.

6. CONCLUSIONS

This study establishes the BEM with linear elements to examine second-order wave interaction with a porous structure in water of finite depth. The accuracy of the proposed BEM is verified by comparing the present numerical results with previous analytical solutions and experimental data. For a low value of relative water depth, the numerical results indicate that second-order components may be important in the region of intermediate depth wave. The second-order components consist of a second-harmonic free-wave and a second-order Stokes' wave. In addition, the wave height of a free-wave is markedly higher than that of a Stokes' wave. Moreover, the fact that the free-wave travels with lower speed down the leeside of the porous structure accounts for why the water surface profile meanders, i.e. surface profiles vary at different positions.

Table I. Media physical properties

C_{f2}	K_{p2} (ft^2)	ε_2 (%)
0.295	0.1138×10^{-5}	0.439
0.282	0.4820×10^{-5}	0.434

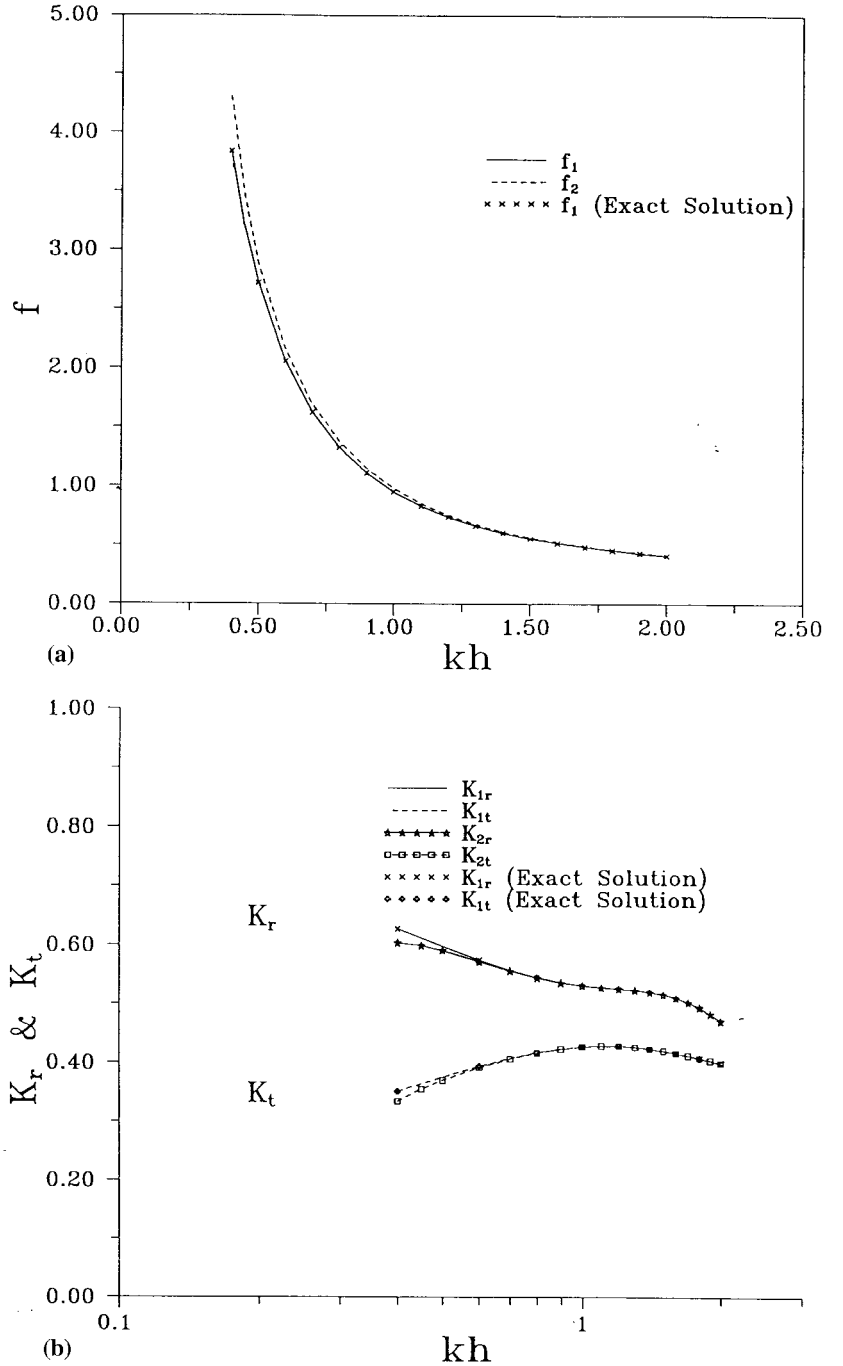

Figure 3. Friction (a), reflection and transmission (b) coefficients ($H/L = 0.01$, $\varepsilon_2 = 0.434$, $K_{p2} = 0.4820 \times 10^{-5}$, $C_{f2} = 0.282$).

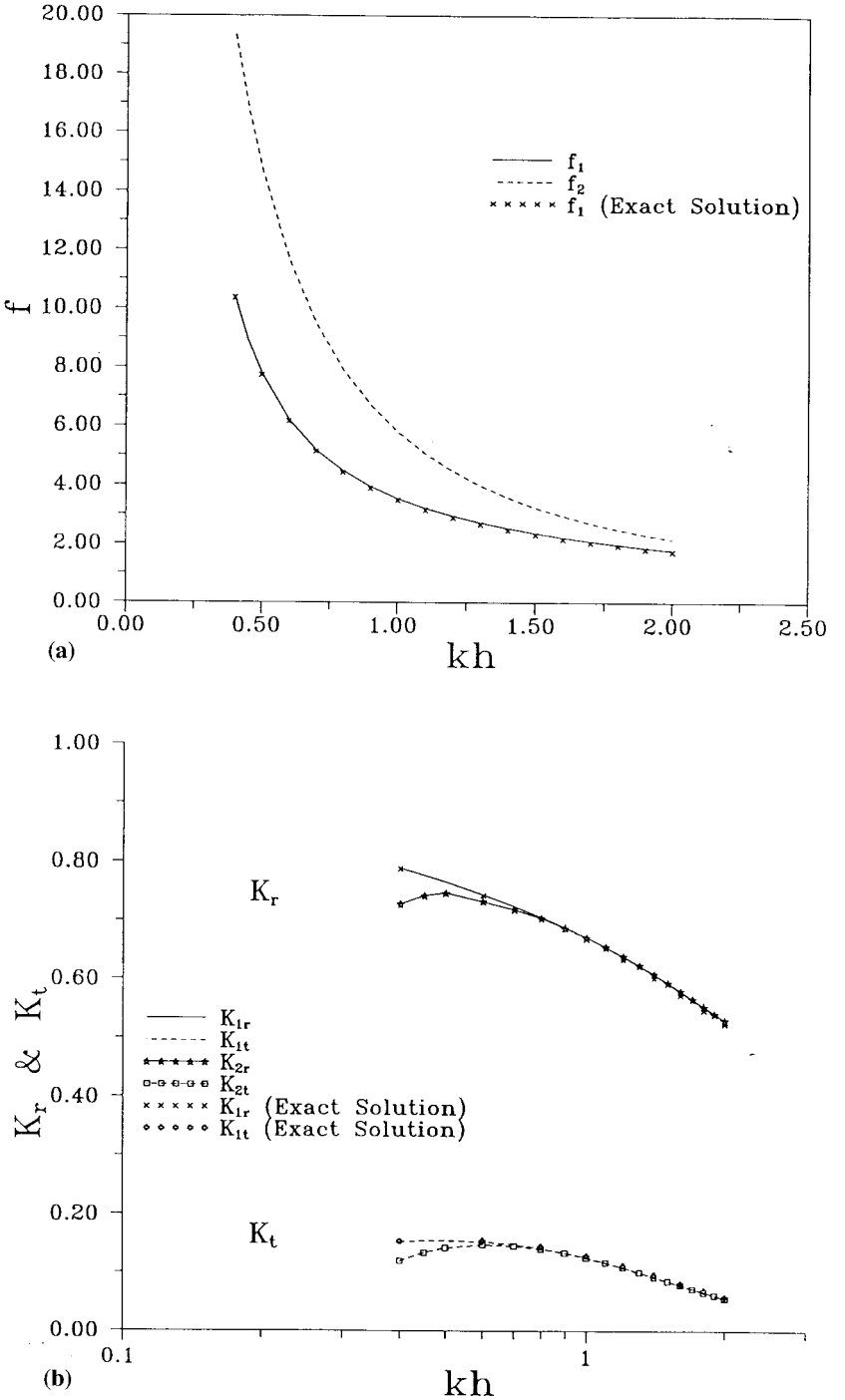

Figure 4. Friction (a), reflection and transmission (b) coefficients ($H/L = 0.02$, $\varepsilon_2 = 0.439$, $K_{p2} = 0.1138 \times 10^{-5}$, $C_{f2} = 0.295$).

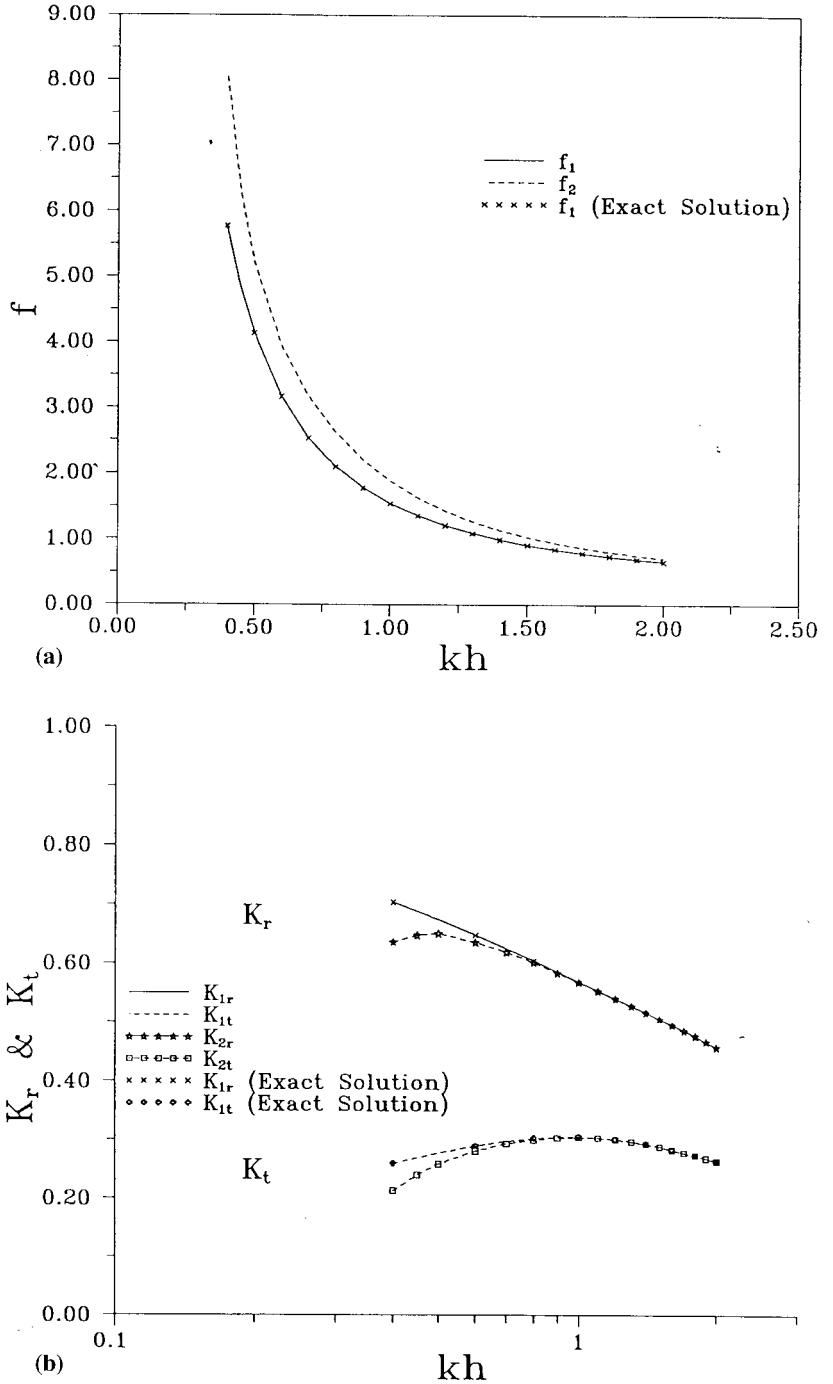

Figure 5. Friction (a), reflection and transmission (b) coefficients ($H/L = 0.02$, $\varepsilon_2 = 0.434$, $K_{p2} = 0.4820 \times 10^{-5}$, $C_{f2} = 0.282$).

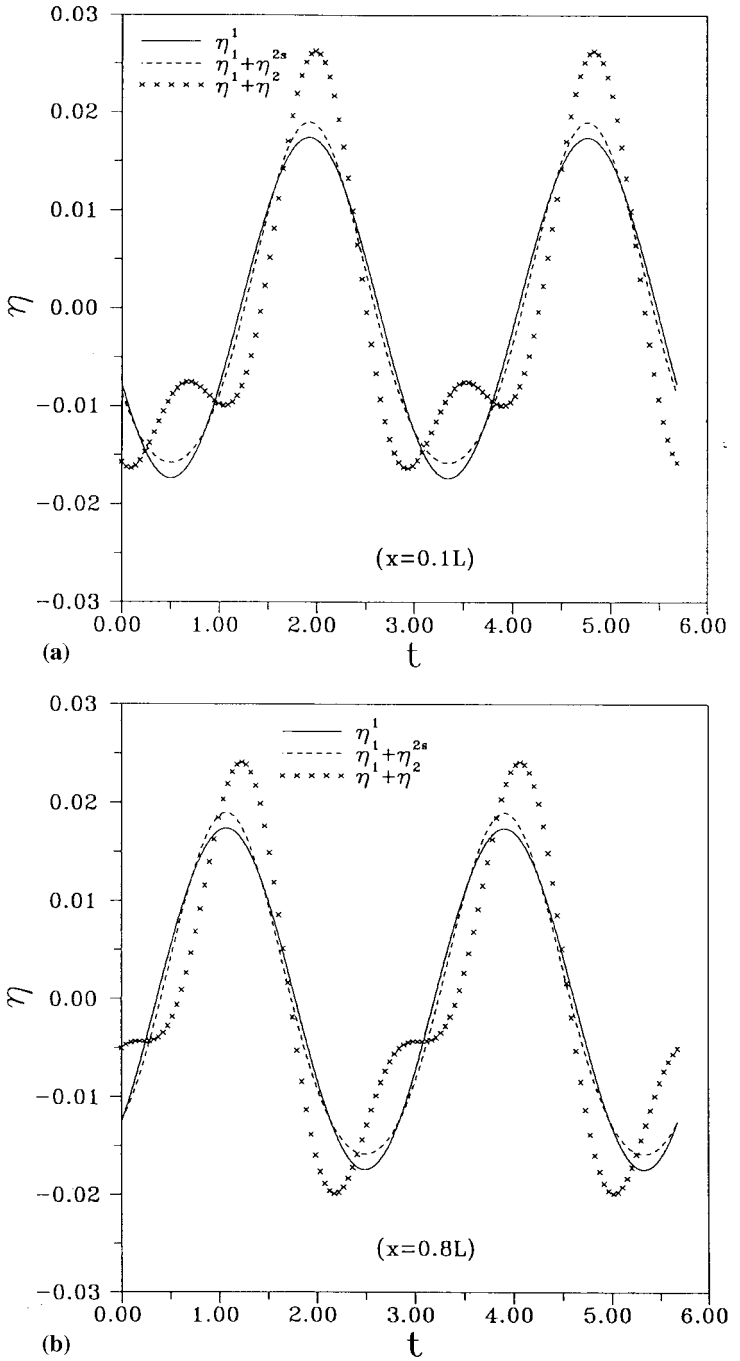

Figure 6. Time variation of the surface elevation at different positions ($H/L = 0.01$, $\varepsilon_2 = 0.439$, $K_{p2} = 0.1138 \times 10^{-5}$, $C_{f2} = 0.295$, $kh = 0.4$).

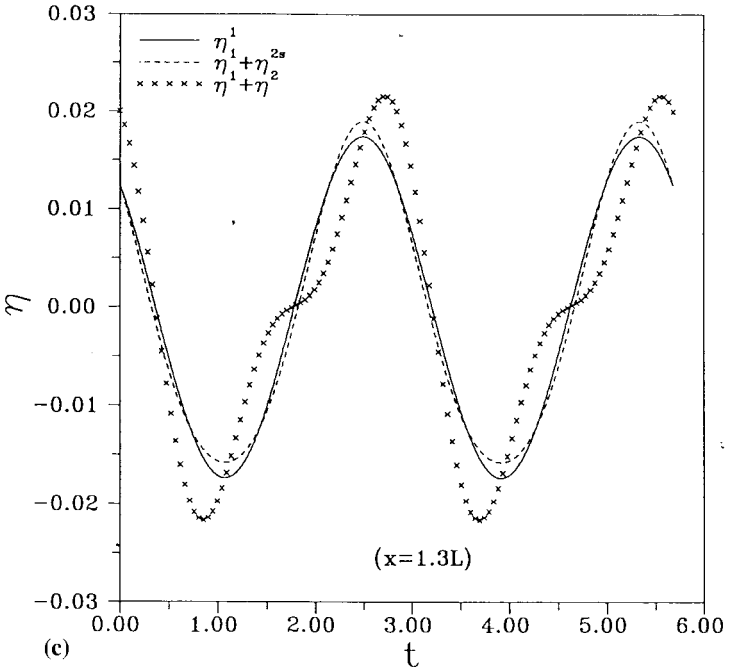

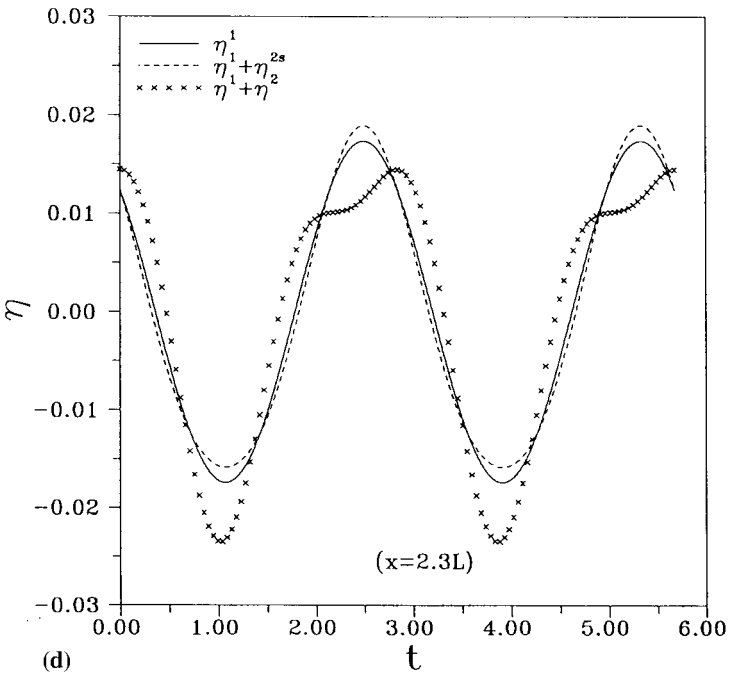

Figure 6 (*Continued*)

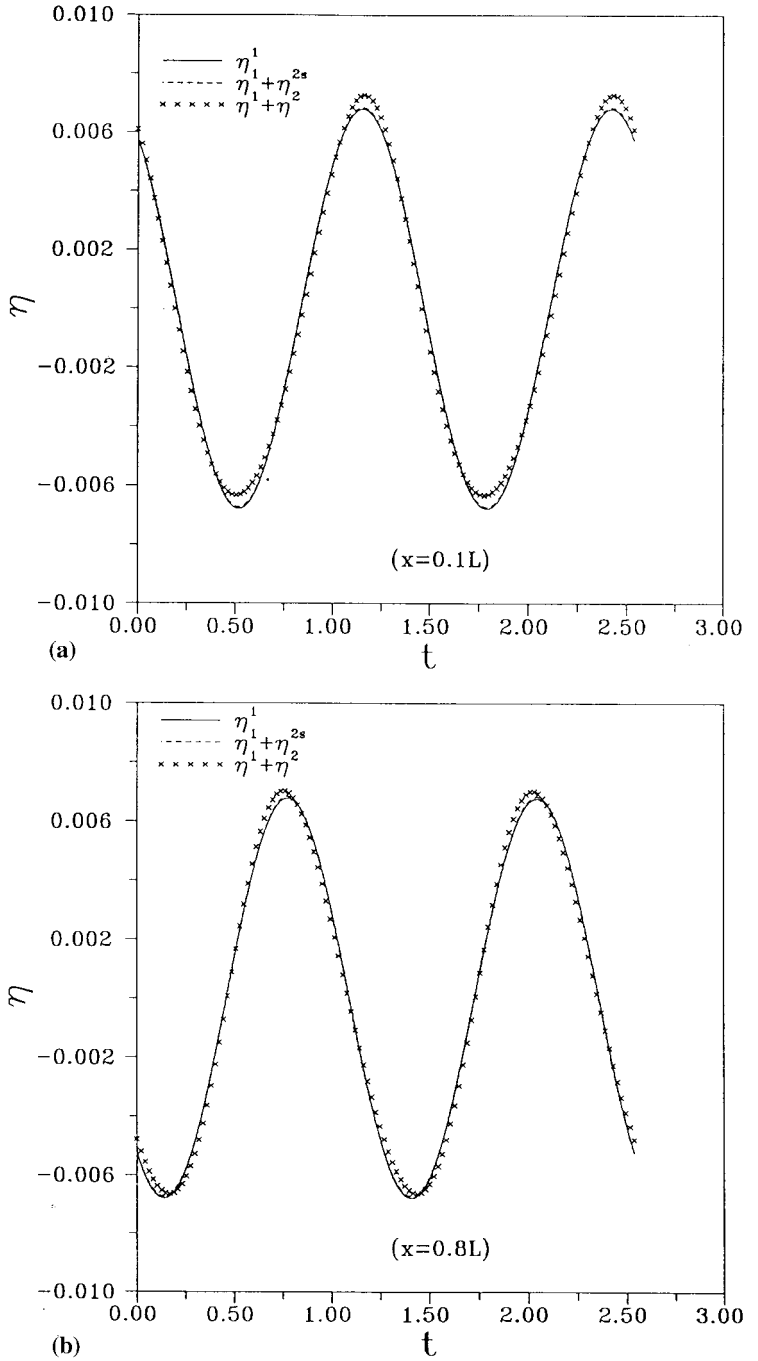

Figure 7. Time variation of the surface elevation at different positions ($H/L = 0.01$, $\varepsilon_2 = 0.439$, $K_{p2} = 0.1138 \times 10^{-5}$, $C_{f2} = 0.295$, $kh = 1.0$).

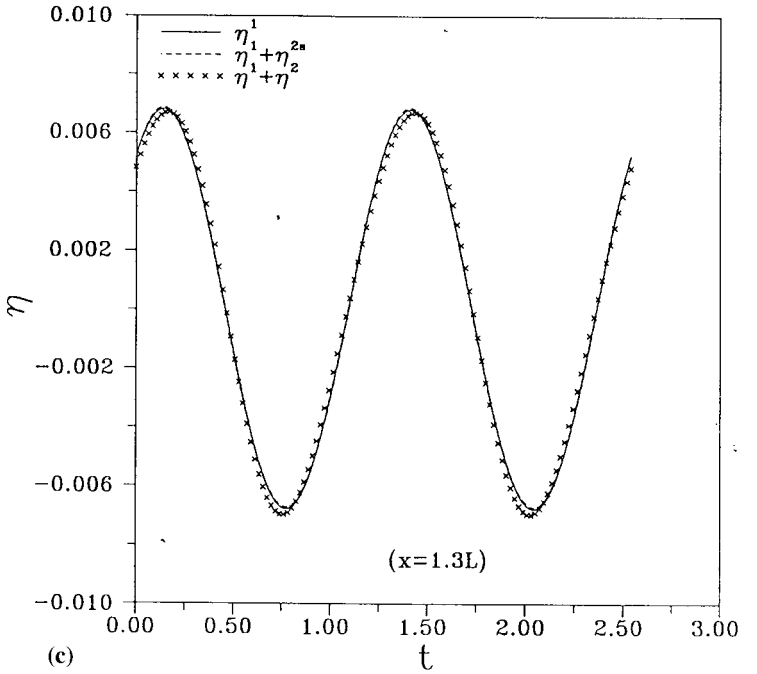

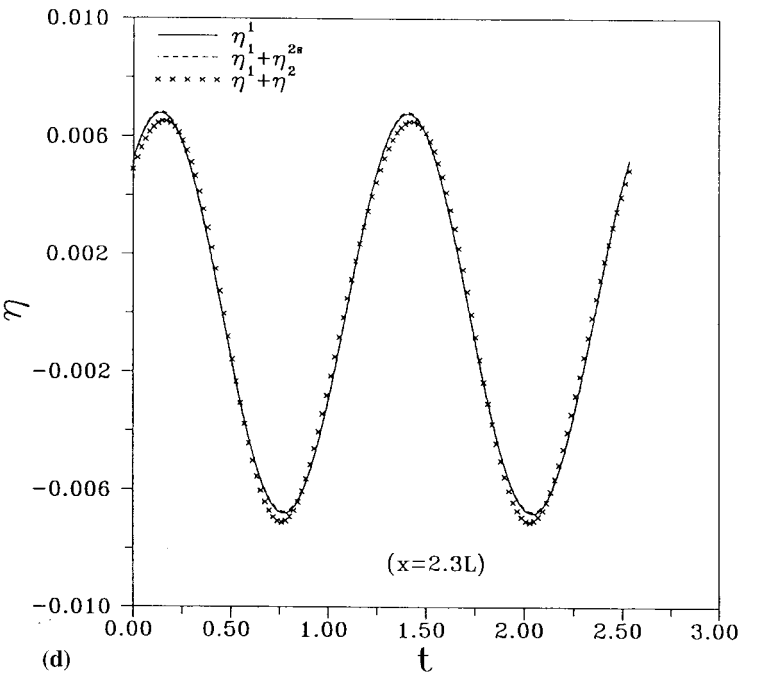

Figure 7 (*Continued*)

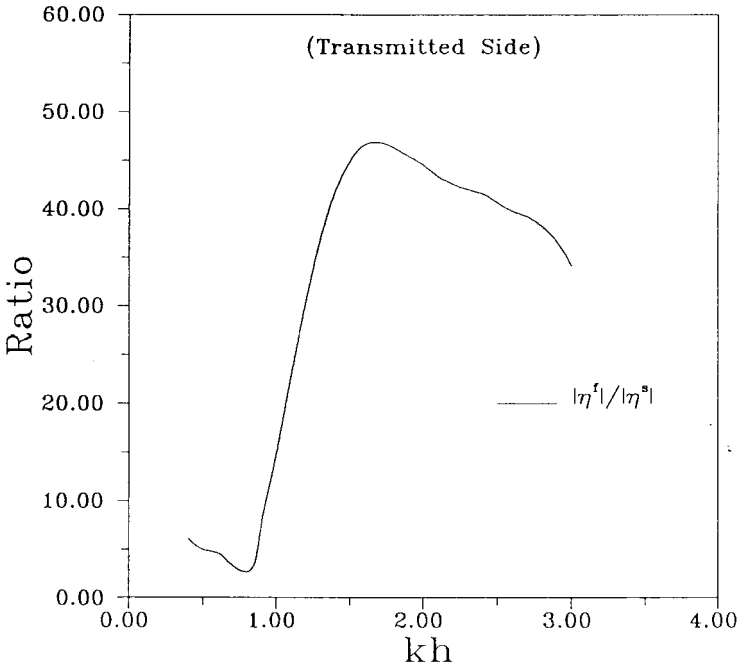

Figure 8. The ratio of second-order wave amplitudes, $|\eta^{2f}/\eta^{2s}|$ ($H/L = 0.01$, $\varepsilon_2 = 0.439$, $K_{p2} = 0.1138 \times 10^{-5}$, $C_{f2} = 0.295$).

ACKNOWLEDGMENTS

The authors would like to thank the National Science Council of the Republic of China for financially supporting this research under Contract No. NSC-85-2611-E-009-001.

APPENDIX A

According to the match conditions of continuity of pressure and horizontal velocity normal to the vertical interface AB and Equation (42), one gets

$$\phi_{11} = \phi_1^{\mathrm{r}} = \frac{g}{2\omega}\frac{\cosh k(h+z)}{\cosh kh}(H + H_{\mathrm{r}}), \tag{67}$$

$$\phi_{11n} = -\phi_{1x}^{\mathrm{r}} = -i\frac{gk}{2\omega}\frac{\cosh k(h+z)}{\cosh kh}(H - H_{\mathrm{r}}). \tag{68}$$

The relationship between ϕ_{11} and ϕ_{11n} on the interface AB can be established as [18]:

$$\phi_{11} = H\frac{g}{\omega}\frac{\cosh k(h+z)}{\cosh kh} + \frac{\cosh k(h+z)}{ikQ_0}\int_{-h}^{0}\frac{\partial\phi_{11}}{\partial n}\cosh k(h+z)\,\mathrm{d}z, \tag{69}$$

where

$$H_{\mathrm{r}} = H + \frac{2\omega\cosh(kh)}{igkQ_0}\int_{-h}^{0}\frac{\partial\phi_{11}}{\partial n}\cosh k(h+z)\,\mathrm{d}z, \tag{70}$$

$$Q_0 = \int_{-h}^{0} \cosh^2 k(h+z)\,\mathrm{d}z. \tag{71}$$

Similarly, on the vertical interface CD,

$$\phi_{31} = \phi_1^{\mathrm{t}} = \frac{gH_{\mathrm{t}}}{2\omega}\frac{\cosh k(h+z)}{\cosh kh}, \tag{72}$$

$$\phi_{31n} = \phi_{1x}^{\mathrm{t}} = i\frac{gkH_{\mathrm{t}}}{2\omega}\frac{\cosh k(h+z)}{\cosh kh}. \tag{73}$$

The relationship between ϕ_{31} and ϕ_{31n} on the interface CD can be established as:

$$\phi_{31} = \frac{\cosh k(h+z)}{ikQ_0}\int_{-h}^{0}\frac{\partial\phi_{31}}{\partial n}\cosh k(h+z)\,\mathrm{d}z, \tag{74}$$

where

$$H_{\mathrm{t}} = \frac{2\omega\cosh(kh)}{igkQ_0}\int_{-h}^{0}\frac{\partial\phi_{31}}{\partial n}\cosh k(h+z)\,\mathrm{d}z. \tag{75}$$

APPENDIX B

According to the match conditions of continuity of pressure and horizontal velocity normal to the vertical interface AB and Equations (46) and (47), one gets

$$\begin{aligned}\phi_{12} = \phi_2^{\mathrm{rs}} + \phi_2^{\mathrm{rf}} = i\left[\frac{gk}{4\omega}\frac{(2\cosh(2kh)-1)}{2\sinh(2kh)}\right]HH_{\mathrm{r}} + (-i)\frac{3\omega}{32}\frac{\cosh[2k(h+z)]}{\sinh^4(kh)}H^2 \\ + (-i)\frac{3\omega}{32}\frac{\cosh[2k(h+z)]}{\sinh^4(kh)}H_{\mathrm{r}}^2 + \bar{A}\cosh\beta(h+z),\end{aligned} \tag{76}$$

$$\phi_{12n} = -\phi_{2x}^{\mathrm{rs}} - \phi_{2x}^{\mathrm{rf}} = -\frac{3k\omega}{16\sinh^4 kh}(H^2 - H_{\mathrm{r}}^2)\cosh 2k(h+z) + i\beta\bar{A}\cosh\beta(h+z). \tag{77}$$

The relationship between ϕ_{12} and ϕ_{12n} on the interface AB can be established as [18]:

$$\phi_{12} = R_1(z) + \frac{-i\cosh\beta(h+z)}{\beta W_0}\int_{-h}^{0}\frac{\partial\phi_{12}}{\partial n}\cosh\beta(h+z)\,\mathrm{d}z, \tag{78}$$

where

$$\bar{A} = \frac{1}{i\beta W_0}\int_{-h}^{0}\frac{\partial\phi_{12}}{\partial n}\cosh[\beta(h+z)]\,\mathrm{d}z + \bar{R}_{\mathrm{L}}, \tag{79}$$

$$W_0 = \int_{-h}^{0}\cosh^2\beta(h+z)\,\mathrm{d}z, \tag{80}$$

$$\bar{R}_{\mathrm{L}} = \frac{1}{i\beta W_0}\int_{-h}^{0}\frac{\partial\phi_2^{\mathrm{rs}}}{\partial x}\cosh[\beta(h+z)]\,\mathrm{d}z, \tag{81}$$

$$R_1(z) = \phi_2^{\mathrm{rs}}(z) + \bar{R}_{\mathrm{L}}\cosh\beta(h+z). \tag{82}$$

Similarly, on the vertical interface CD,

$$\phi_{32} = \phi_2^{ts} + \phi_2^{tf} = \frac{-i3\omega}{32\sinh^4 kh} H_t^2 \cosh 2k(h+z) + \bar{B}\cosh\beta(h+z), \tag{83}$$

$$\phi_{32n} = \phi_{2x}^{ts} + \phi_{2x}^{tf} = \frac{3k\omega}{16\sinh^4 kh} H_t^2 \cosh 2k(h+z) + i\beta\bar{B}\cosh\beta(h+z). \tag{84}$$

The relationship between ϕ_{32} and ϕ_{32n} on the interface CD can be established as:

$$\phi_{32} = R_2(z) + \frac{-i\cosh\beta(h+z)}{\beta W_0}\int_{-h}^{0} \frac{\partial\phi_{32}}{\partial n}\cosh\beta(h+z)\,\mathrm{d}z, \tag{85}$$

where

$$\bar{B} = \frac{1}{i\beta W_0}\int_{-h}^{0} \frac{\partial\phi_{32}}{\partial n}\cosh[\beta(h+z)]\,\mathrm{d}z + \bar{R}_R, \tag{86}$$

$$\bar{R}_R = \frac{-1}{i\beta W_0}\int_{-h}^{0} \frac{\partial\phi_2^{rs}}{\partial x}\cosh[\beta(h+z)]\,\mathrm{d}z, \tag{87}$$

$$R_2(z) = \phi_2^{rs}(z) + \bar{R}_R\cosh\beta(h+z). \tag{88}$$

REFERENCES

1. C.K. Sollitt and R.H. Cross, 'Wave transmission through permeable breakwaters', in *Proc. 13th Int. Conf. on Coastal Engineering*, Vancouver, ASCE, **III**, 1837–1846 (1972).
2. O.S. Madsen, 'Wave transmission through porous structures', *J. Waterway Port Coast. Ocean Eng. Div. ASCE*, **100**, 169–188 (1974).
3. O.S. Madsen and S.M. White, 'Reflection and transmission characteristics of porous rubble-mound breakwaters', *Miscellaneous Report No. 76-5*, US Army, Coastal Engineering Research Center, 1976.
4. C.P. Lee, Wave interaction with permeable structures, *Ph.D. Thesis*, Oregon State University, Corvallis, OR, 1987.
5. R.A. Dalrymple, M.A. Losada and P.A. Martin, 'Reflection and transmission from porous structures under oblique wave attack', *J. Fluid Mech.*, **224**, 625–644 (1991).
6. J.F. Lee and Y.J. Lan, 'A second-order solution of waves passing porous structures', *Ocean Eng.*, **23**, 143–165 (1996).
7. W. Sulisz, 'Wave reflection and transmission at permeable breakwaters of arbitrary cross-section', *Coast. Eng.*, **9**, 371–386 (1985).
8. A.T. Chwang, 'A porous-wavemaker theory', *J. Fluid Mech.*, **132**, 395–406 (1983).
9. G.I. Taylor, 'Fluid flow in regions bounded by porous surface', *Proc. R. Soc.*, **A234**, 456–475 (1956).
10. L.H. Huang and H.I. Chao, 'Reflection and transmission of water-wave by porous breakwater', *J. Waterway Port Coast. Ocean Eng. Div. ASCE*, **118**, 437–451 (1992).
11. T. Iwasaki and A. Numata, 'Experimental studies on wave transmission of a permeable breakwater constructed by artificial blocks', *Coast. Eng. Jpn.*, **13**, 25–29 (1970).
12. J. Dattari, H. Raman and J.N. Shankar, 'Performance characteristic of submerged breakwaters', in *Proc. 16th Coast. Eng. Conf. ASCE*, Hamburg, 2153–2171 (1978).
13. P. Aminti and L. Franco, 'Wave overtopping on rubble-mound breakwaters', in *Proc. Int. Conf. on Coastal Engineering*, Malaga, ASCE, 770–781 (1988).
14. H. Oumeraci and H.W. Partenscky, 'Wave-induced pore pressure in rubble-mound breakwater', in *Proc. Int. Conf. on Coastal Engineering*, Delft, ASCE, 1334–1347 (1990).
15. H.A. Lorentz, *Report of the State Committee Zuidersee 1918–1926, (Dutch Text)*, Den Haag, Alg, Landsdrokkerij, 1926.
16. R.G. Dean and R.A. Dalrymple, *Water Wave Mechanics for Engineers and Scientists*, Prentice-Hall, Englewood Cliffs, NJ, 1984.
17. M. Vantorre, 'Third-order theory for determining the hydrodynamic forces on axisymmetric floating or submerged bodies in oscillatory heaving motion', *Ocean Eng.*, **13**, 339–371 (1986).
18. Y.C. Wu, 'Analysis of wave fields generated by a directional wavemaker', *Coast. Eng.*, **11**, 241–261 (1987).
19. T.I. Kim, 'Mass transport in laboratory water-wave flumes', *Ph.D. Thesis*, Oregon State University, OR, 1984.
20. C.A. Brebbia and J. Dominguez, *Boundary Elements: An Introductory Course*, McGraw-Hill, New York, 1989.
21. M.D. Greenberg, *Application of Green's Function in Science and Engineering*, Prentice-Hall, Englewood Cliffs, NJ, 1971.

